IMPLEMENTATION OF THE DEVIATION OPERATOR

Özdoğan Yılmaz and Jon F. Claerbout

The deviation operator (Dev) is defined as the error made in separating the double square root operator (DS) (see Claerbout and Yılmaz, this report). A second order approximation to the deviation operator yields an equation that can easily be implemented. Conventional data processing can be considerably improved by applying this operator to common offset sections prior to NMO correction. The process tends to correct for dipping events; thus, together with the NMO, each common offset section is more accurately mapped onto a zero-offset section. Models of point scatterers at different depths in (a) a constant velocity medium and (b) a medium with vertically varying velocity were used to test the deviation operator. Results indicate that, following the application of the deviation operator, the success of imaging common offset sections is comparable to that of zero-offset sections.

Background

Conventional data processing utilizes the separable form of the double square root operator. Theoretical analysis of the error involved in separation is made in another paper by Claerbout and Yılmaz, in this report. The error is formally defined as the difference between the double square root operator and its separable form

$$\mathrm{Dev}(Y,\hat{H}) = \mathrm{DS}(Y,\hat{H}) - \mathrm{Sep}(Y,\hat{H}) \tag{1}$$

where $\hat{H}$ is some estimate of H. The operator Sep(Y,H) contains two parts: one is a zero-dip, NMO-type operator, and the other is a zero-offset migration operator. As a matter of fact, what we just described is conventional processing. The zero-dip assumption can be relaxed by applying the deviation operator $Dev(Y,\hat{H})$ prior to $Sep(Y,H)$.

Let us now have a closer look at the deviation operator. Making all the relevant substitutions, (1) takes the form

$$Dev(Y,\hat{H}) = [1 - (Y - \hat{H})^2]^{1/2} + [1 - (Y + \hat{H})^2]^{1/2} - 2[(1 - Y^2)^{1/2} + (1 - \hat{H}^2)^{1/2} - 1] \quad (2)$$

Equation (2) is rather formidable, and besides, a second order approximation in dip would suffice for the accuracy required. As derived in the previous paper, the approximate deviation operator is

$$Dev(Y,\hat{H}) \approx [1 - (1 - \hat{H}^2)^{-3/2}]\, Y^2 \quad (3)$$

A further consideration that comes up is an estimate for $\hat{H}$. What we would really like to do is to apply the operator given by (3) to each common offset section, independently. In fact, a suitable choice for $\hat{H}$ is

$$\hat{H} = \frac{2h}{v_{RMS}\, t} \quad (4)$$

where h is the surface offset and t is the observation time, also measured from the surface. Equation (4) is derived from ray-theoretical considerations (Claerbout, SEP-15, pp. 57-71). Substituting (4) into (3) and incorporating the missing factor $-\omega/v$, we get

$$\omega k_z = -\frac{\tilde{v}}{4} k_y^{\,2} \quad (5a)$$

where

$$\tilde{v} = v_{int}\left\{1 - \left[1 - \left(\frac{2h}{v_{RMS}t}\right)^2\right]^{-3/2}\right\} \tag{5b}$$

Notice that (5a) is in the form of the retarded 15-degree approximation to the zero-offset migration equation. The difference is that the extrapolation velocity in (5a) is not the medium velocity but the one defined by (5b). Moreover, since $\hat{H}$ is the sine of offset angle ($\hat{H} \leq 1$), the factor multiplying v_{int} in (5b) is a negative quantity. Keeping this in mind, the corresponding partial differential equation is

$$P_{zt} = \frac{\tilde{v}}{4} P_{yy} \quad , \qquad \tilde{v} < 0 \tag{6}$$

Finally, referring to (5b), $\tilde{v}$ can be considered as the velocity of propagation adjusted for offset.

Our old friend, the 15-degree computational star, can be used if v_{int} is changed to $\tilde{v}$. The t-outer algorithm was used in the present analysis for two reasons: (a) less memory is required, and (b) more important, $\hat{H}$ is constant along the extrapolation path $t = \text{const}$.

Equation (6) can also be used for the case of a medium with a velocity varying vertically. It is convenient, however, to make the conversion

$$\tau = 2 \int \frac{dz}{v_{int}} \tag{7}$$

which yields

$$P_{\tau t} = \frac{\tilde{\tilde{v}}}{4} P_{yy} \quad , \qquad \tilde{\tilde{v}} < 0 \tag{8}$$

where

$$\tilde{\tilde{v}} = \frac{v_{int}^2}{2}\left\{1 - \left[1 - \left(\frac{2h}{v_{RMS}t}\right)^2\right]^{-3/2}\right\} \tag{9}$$

The output from (8) is collected along the diagonal $\tau = t$. Care should be given to the fact that $v_{int} = v_{int}(\tau)$ and $v_{RMS} = v_{RMS}(t)$.

A final consideration is that Equation (8) has a pole at $t = 2h/v_{RMS}$, which seems worrisome. However, we may stop the extrapolation at this time for two reasons: (a) angles become large so that our equation does not handle them properly; and (b) non-zero data for $t < 2h/v_{RMS}$ would not fit a wave propagation model.

Model experiments

Common offset sections with $h = 0$ and $h = 400$ m (Figures 2a,b and 6a,b) were computed via ray-path integral equations over a medium with constant velocity (Figure 1) and a medium with velocity varying vertically (Figure 5). Non-zero-offset sections, after being processed by the deviation operator (Dev), are shown in Figures 3 and 7. A practical test of the effect of the Dev process would be to migrate the non-zero-offset sections and compare the results with the migrated zero-offset sections. Figures 4a,b,c and 8a,b,c clearly demonstrate the superior results obtained from the processing sequence that includes the Dev operator. Here, we used the 15-degree migration scheme for the sake of convenience. Certainly, other schemes, such as the 45-degree or the f-k, can be used for better imaging. It is instructive to note that no dip filtering was done during migration, so that the Dev process can be analyzed in an unbiased fashion.

Conclusions

We have demonstrated the improvement of the conventional processing by the deviation operator. As for the computational cost, it is no different from the 15-degree differencing star. In fact, it is apparent that the Dev operator does less to the data than the zero-offset 15-degree migration operator. Therefore, computational cost can be reduced considerably by extrapolating with a small number of z-steps. While going up the section, this number can be gradually increased, thus necessitating some kind of interpolation. Results of the experiments with variable z-steps (as a function of t) are shown in Figures 9 and 10. As to the placement of the Dev process in the conventional processing flow diagram, it should be applied before NMO, since the conventional NMO is based on a zero-dip assumption.

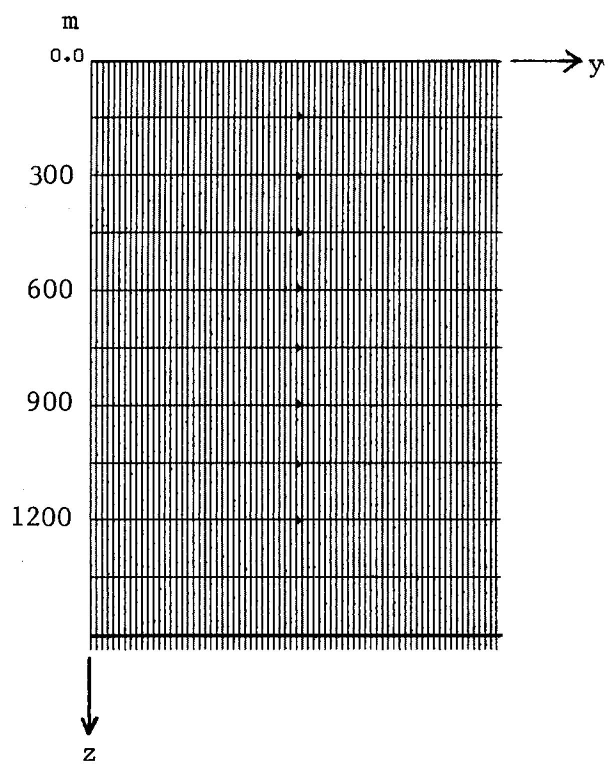

FIGURE 1.--Constant velocity model (v = 3000 m/sec). Eight point scatterers buried at depths between z = 150-1200 m.

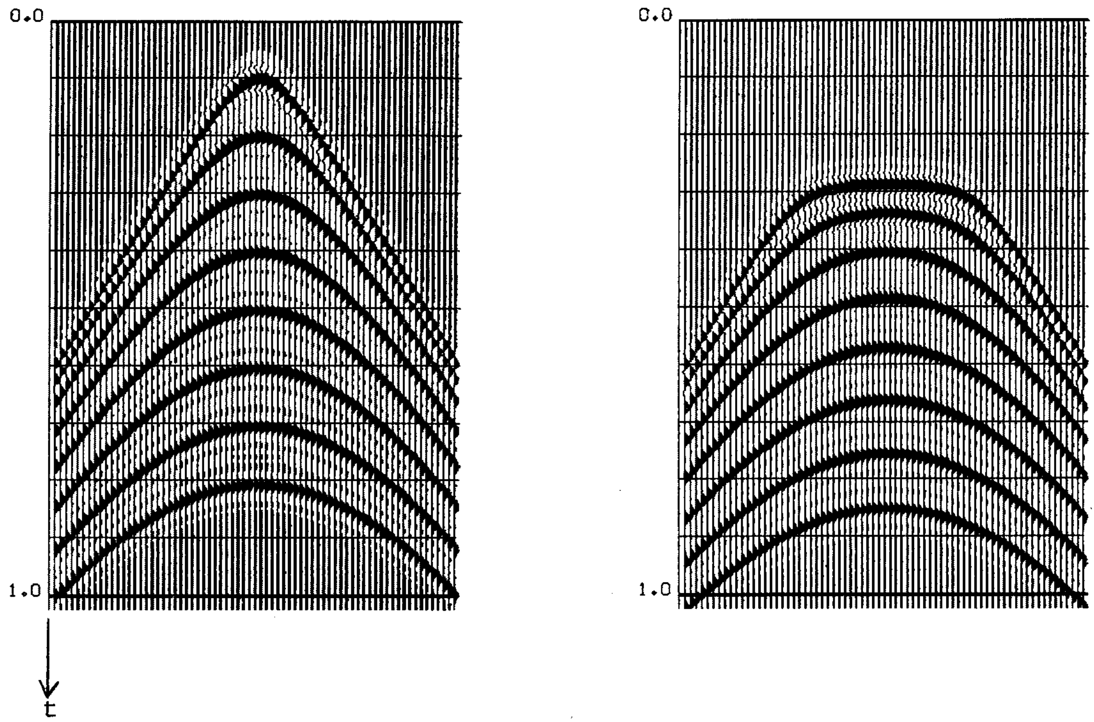

2a 2b

FIGURE 2.--Synthetic common offset sections for the model in Figure 1; (a) h = 0, (b) h = 400 m. Note the flattening top of the shallow event in (b). $\Delta t = 0.008$ sec and bandwidth is 6, 12-36, 48 Hz. Amplitudes decay as $t^{-1/2}$.

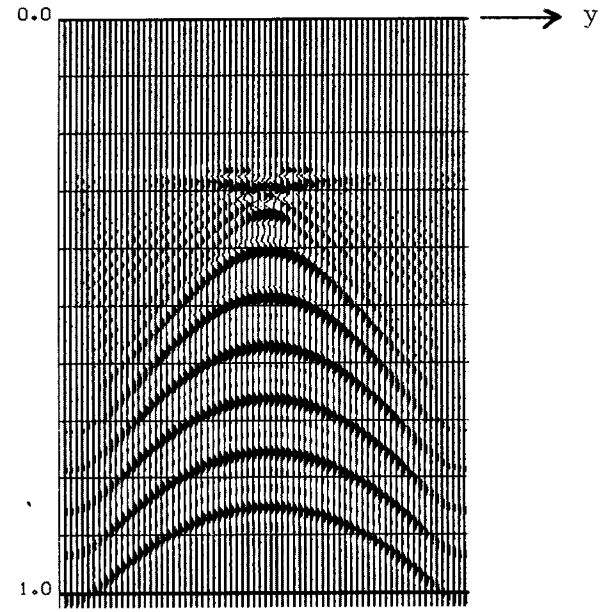

3

FIGURE 3.--Result of applying the deviation operator [Equation (6)] to the common offset section of Figure 2b. Dispersion arises from the top event, which is just below the pole $t = 2h/v_{RMS}$. Theoretically, a great number of steps are required to accurately handle the data near the pole. Note how other pseudo-hyperbolae have been compressed.

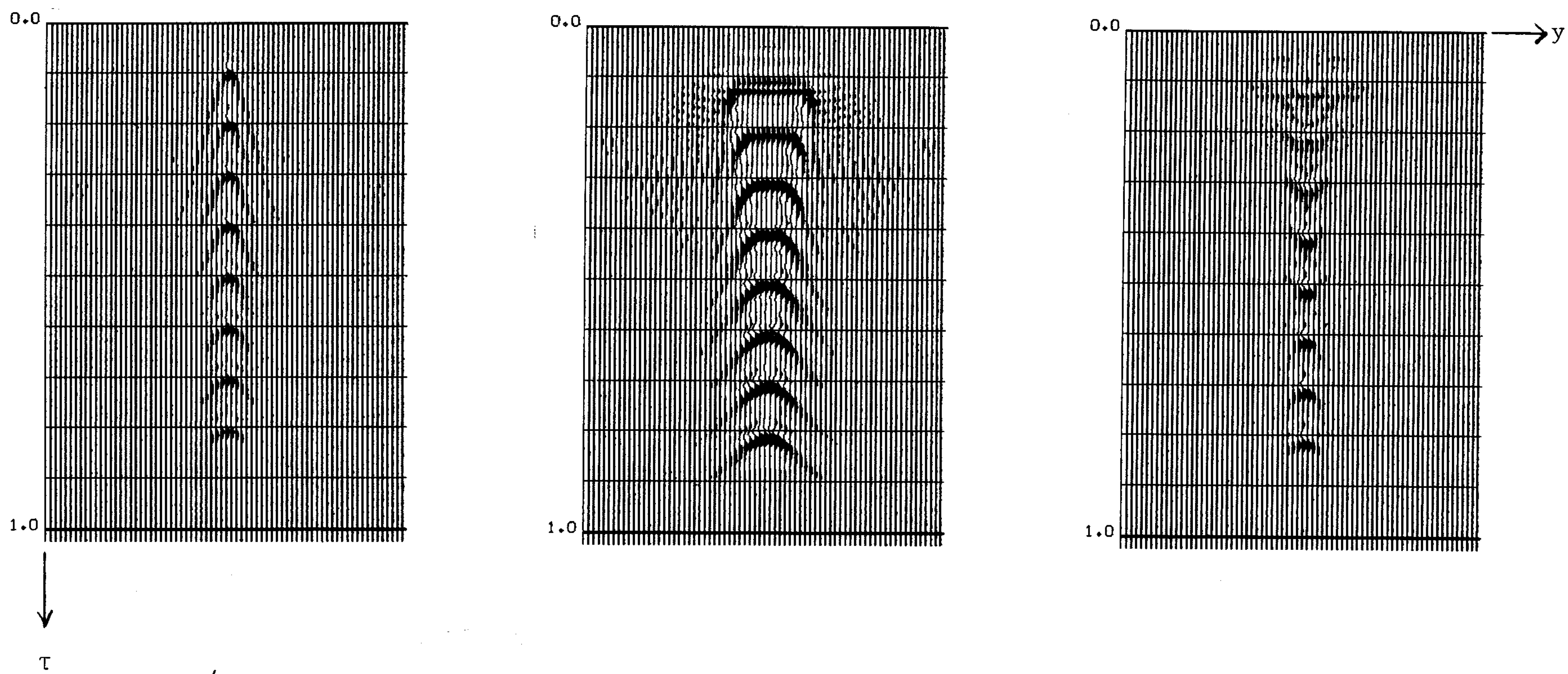

4a 4b 4c

FIGURE 4.--Results of migrating common offset sections (Figures 2a,b) with the 15-degree finite difference scheme. (a) Zero-offset section after migration, (b) common offset section (h = 400 m) after NMO and migration = Sep, (c) common offset section (h = 400 m) after Dev + NMO and migration. Notice the poor result obtained from migrating the common offset section (h = 400 m) without the deviation operator. Subsequent stacking of (a) and (b) would not yield an image as crisp as that obtained from stacking (a) and (c).

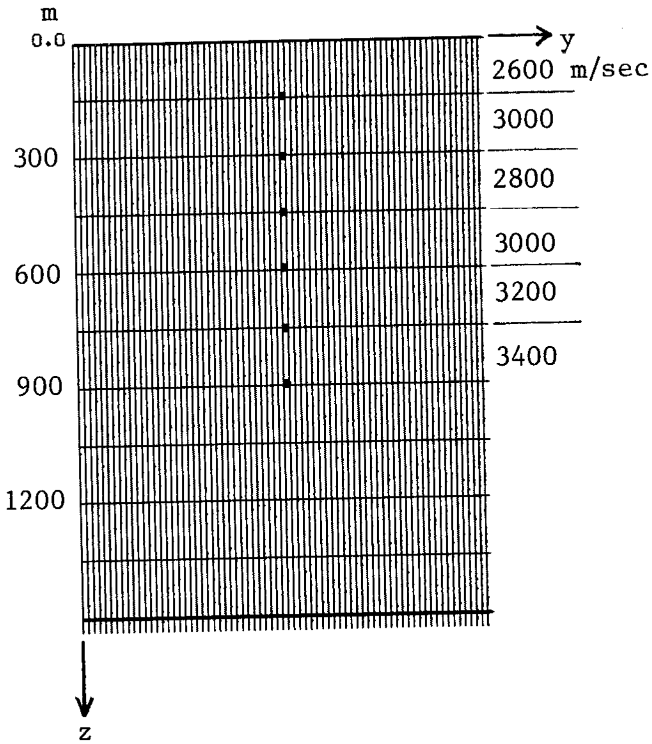

5a

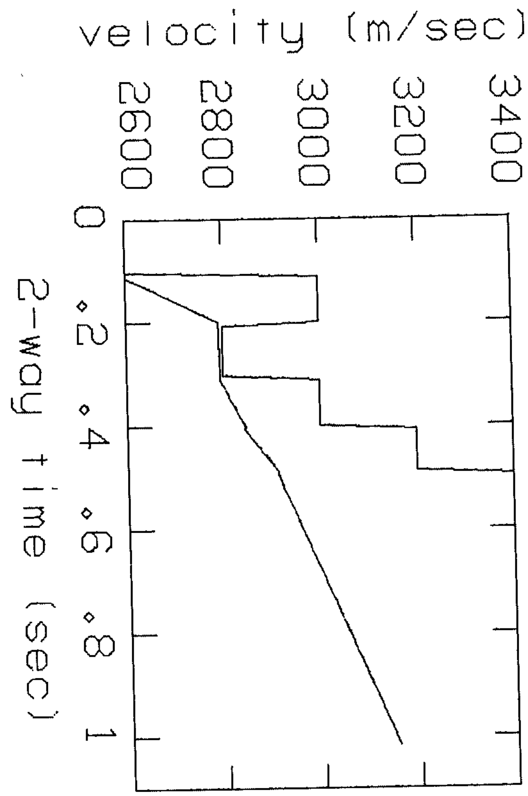

5b

FIGURE 5.--Variable velocity v(z) model. (a) Six point scatterers buried at depths between z = 150-900 m. (b) RMS and interval velocities as a function of traveltime.

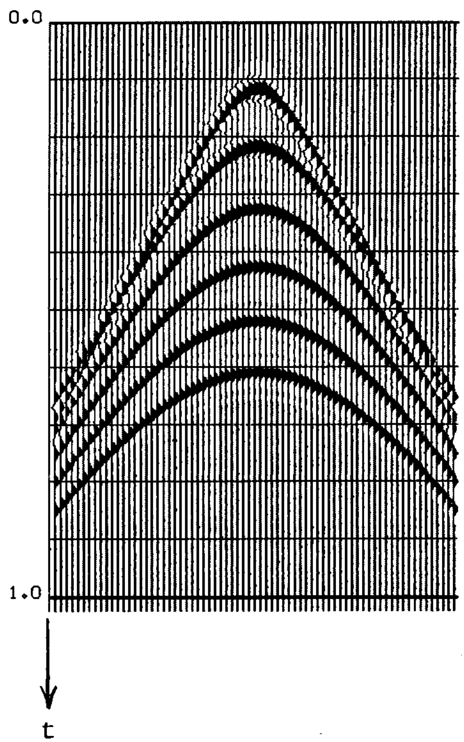

6a

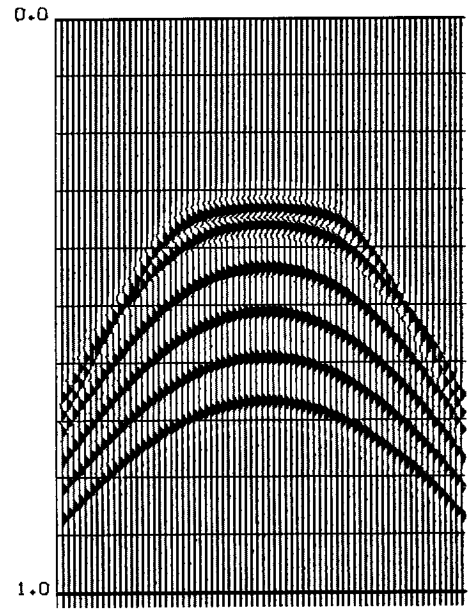

6b

FIGURE 6.--Synthetic common offset sections for the model in Figure 5a. (a) h = 0, (b) h = 400 m. $\Delta t = 0.008$ sec and bandwidth is 6, 12-36, 48 Hz. Amplitudes decay as $t^{-1/2}$.

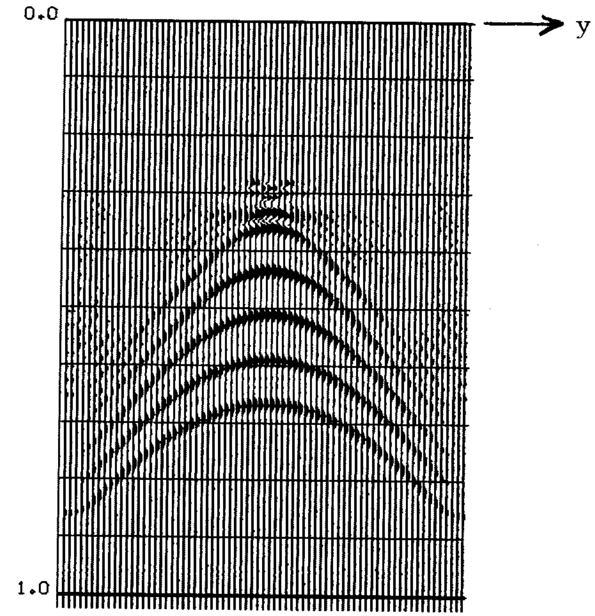

7

FIGURE 7.--Result of applying the deviation operator [Equation (8)] onto the common offset section of Figure 6b.

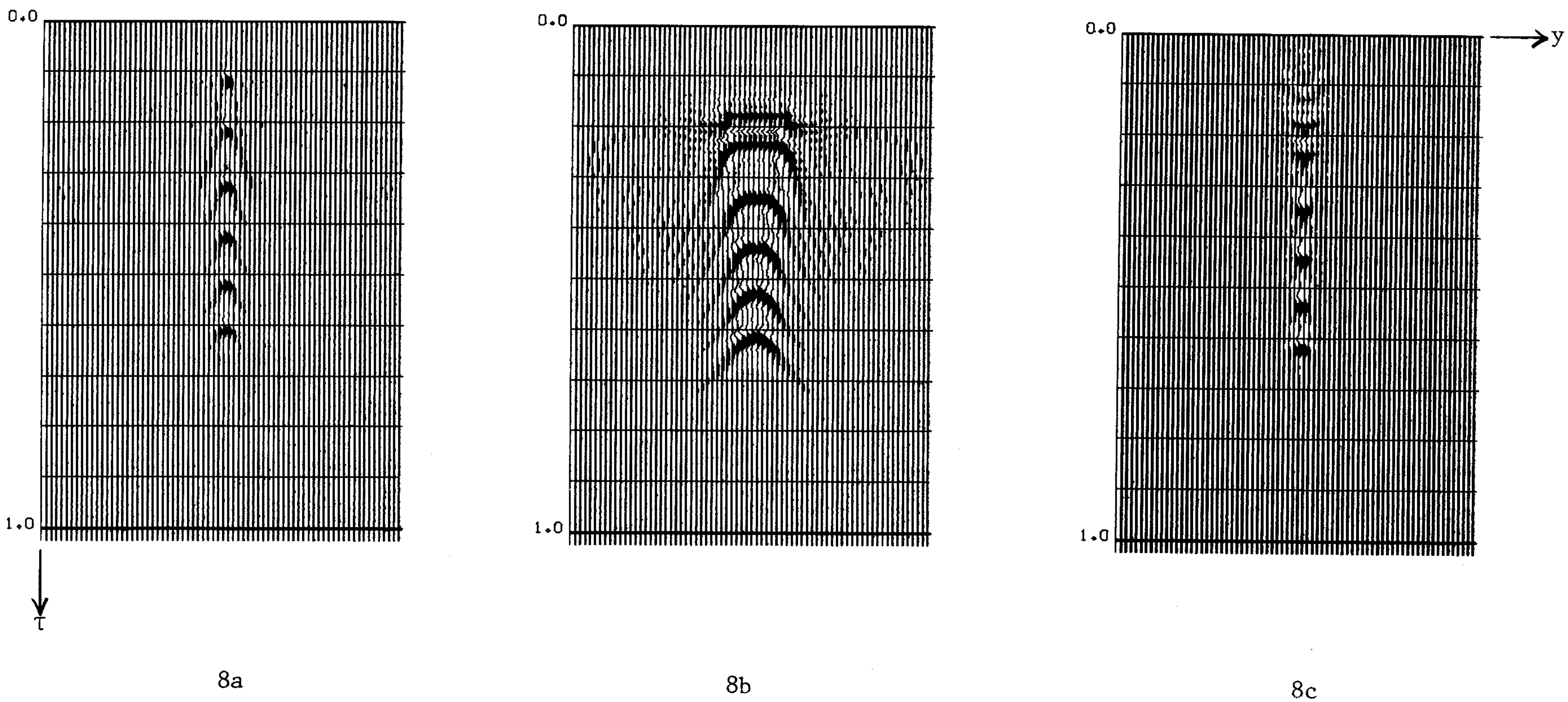

FIGURE 8.--Results of migrating common offset sections (Figures 6a,b) with the 15-degree finite difference scheme. (a) Zero-offset section after migration; (b) common offset section (h = 400 m) after NMO and migration = Sep; (c) common offset section (h = 400 m) after Dev + NMO and migration. Again, the crisp imaging of the non-zero-offset section is achieved by first applying the deviation operation (Dev) prior to conventional processing (Sep).

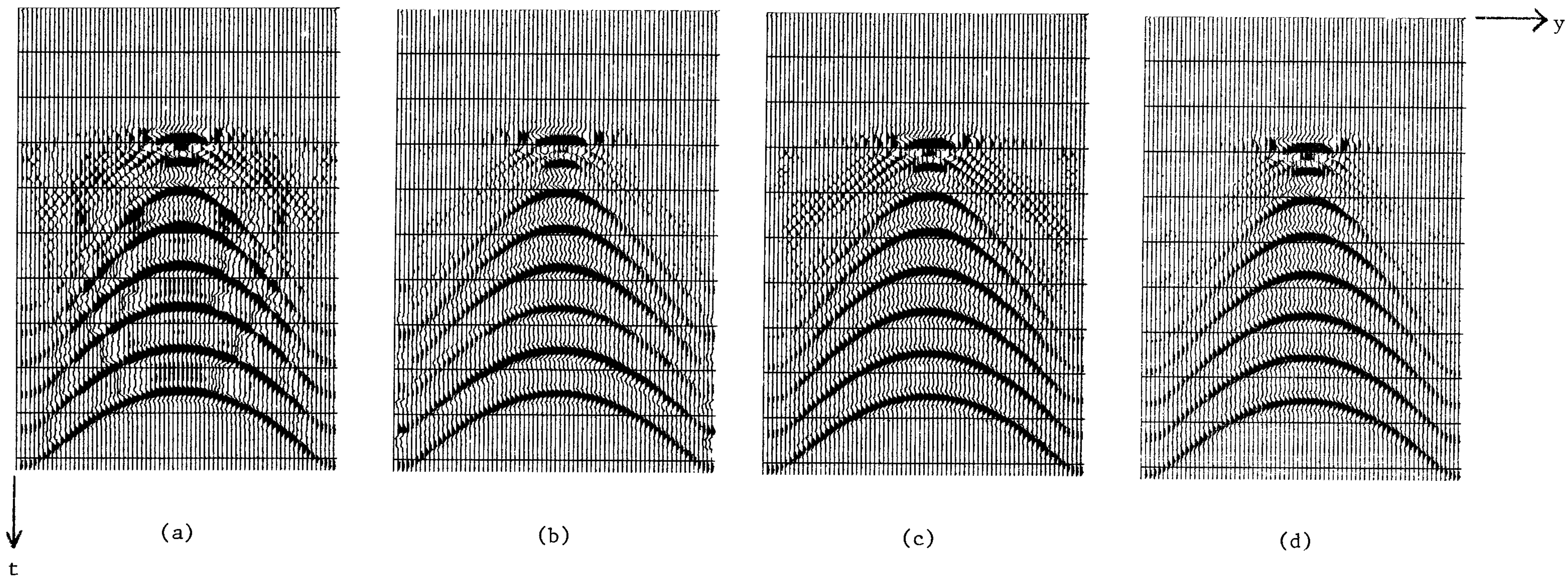

FIGURE 9.--Illustrating possible means of interpolation required during resampling of the (z,y)-plane with a different $z(t)$. (a) Nearest neighbor, (b) linear interpolation, (c) 4-point Lagrangian, (d) cubic spline. Note the two types of undesired effects, namely the frequency dispersion and the noise generated from bad numerical technique for interpolation. The first effect can be eliminated by a denser sampling of the wavefield (Figure 10). The second effect is quite prominent in the nearest neighbor technique for interpolation. The most desirable type of interpolation is Lagrangian or cubic spline.

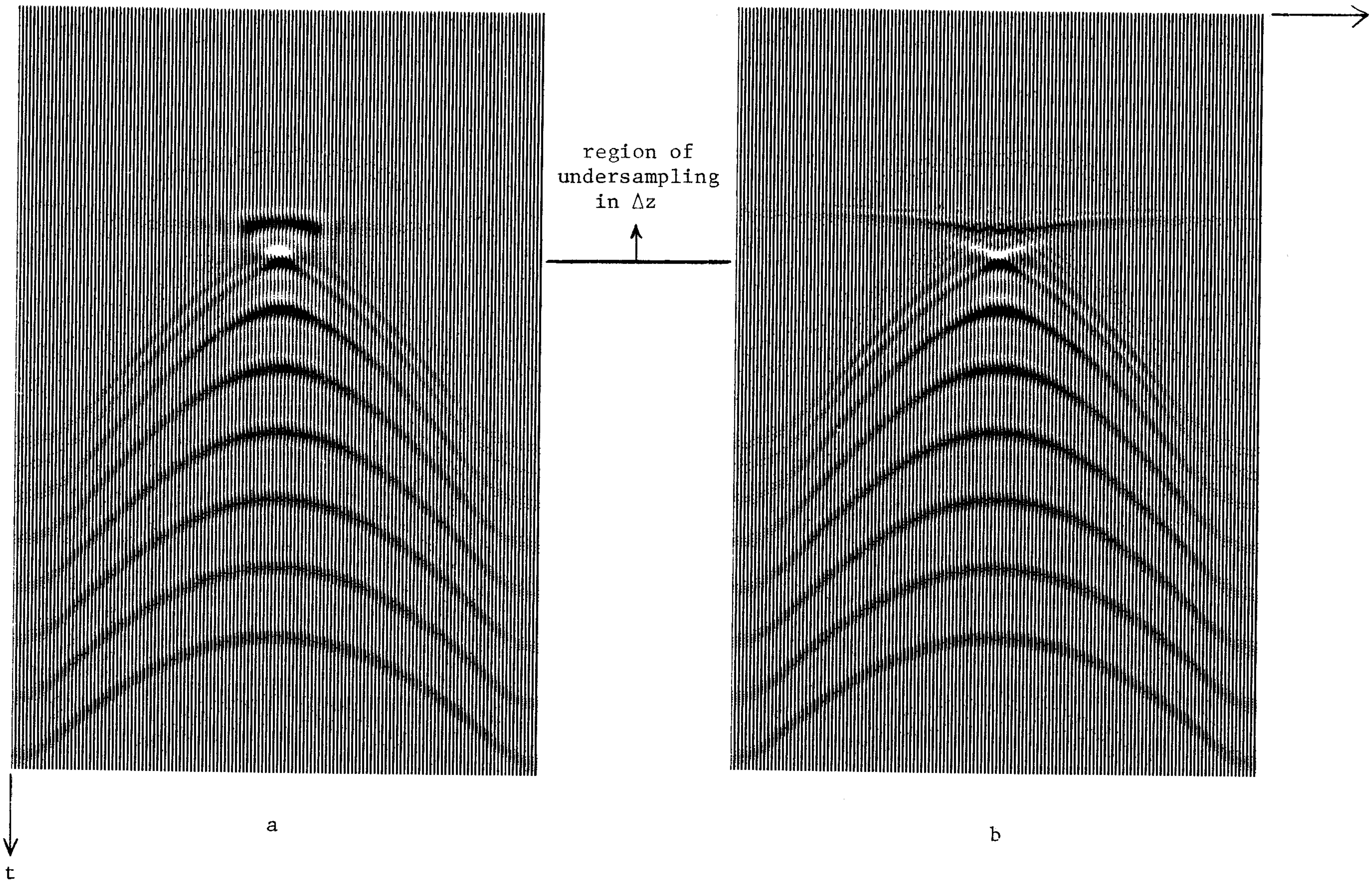

FIGURE 10.--Deviation operator applied on the same data of Figure 2b, but with Δt = 4 msec and Δy = 12.5 m, thus twice the density in both t and y. Both in (a) and (b), number of z-steps is t-dependent, increasing as one goes up the section. Limitation on the maximum number of z-steps caused the under-processing of the data above the line as in (a). By choosing coarser Δz-steps in this region, we can cure this problem, now creating, however, more dispersion as in (b).